https://doi.org/10.5194/egusphere-2025-4589
Preprint. Discussion started: 5 October 2025

Attributing the decadal variations in springtime East Asian and North American dust emission to regime shifts in extratropical cyclone

Yiting Wang[1], Yan Yu[1,2,3], Ji Nie[1,2,3], Bing Pu[4]

[1]Department of Atmospheric and Oceanic Sciences, School of Physics, Peking University, Beijing, China
[2]Laboratory for Climate and Ocean-Atmosphere Studies, Department of Atmospheric and Oceanic Sciences, School of Physics, Peking University, Beijing, China
[3]China Meteorological Administration Tornado Key Laboratory
[4]Department of Geography and Atmospheric Science, University of Kansas, Lawrence, KS, USA
*Correspondence to Yan Yu (yuyan@pku.edu.cn) and Ji Nie (jinie@pku.edu.cn)

Abstract

Dust activities across East Asia and North America have shown decadal variations, mediating radiation budget, air quality, and human health, especially during their peak months of April and May. Using satellite and ground measurements, as along with simulations from a dust emission model, we demonstrate an increase of 3.6% and 30.1% in April dust emissions across East Asia and North America, respectively, during the past four decades, in contrast to a 30.6% and 13.3% decrease during the last two decades. Meanwhile, both regions show a steady increase in May dust emissions by 28.8% and 20.0%, respectively, since the 1980s. Sensitivity experiments attribute both regions' decadal variations in dust emission primarily to surface wind speed changes; whereas vegetation exerts minimum influence on the regional dust emission variations. Furthermore, these decadal variations in dust initiating wind could largely be attributed to regime shifts in extratropical cyclone (EC), including their duration and intensity. These results highlight the changing frequency and duration of strong winds, especially those associated with EC, in shaping the decadal variations of mid-latitude dust emissions.

1. Introduction

East Asia and North America are significant dust source regions in the Northern Hemispheric mid-latitudes. The presence and transportation of dust alter the radiation budget (Adebiyi et al., 2023;

https://doi.org/10.5194/egusphere-2025-4589
Preprint. Discussion started: 5 October 2025

Chen et al., 2013; Huang et al., 2014) and biogeochemical cycles of the marine and terrestrial ecosystems (Jickells and Moore, 2015; Kong et al., 2022; Jickells et al., 2005). Apart from the influence on the natural environment, extreme dust activities also impair atmospheric visibility, air quality, and human health across downwind regions, including populated areas in China and the United States (Gui et al., 2022; Hashizume et al., 2020; Yang et al., 2015). These environmental and societal concerns of dust activity peak in April and May across both regions, when vegetation and snow provide insufficient protection of the dry soil, accompanied by strong near-surface winds and frequent extratropical cyclones (Aryal and Evans, 2022; Kim et al., 2017; Kurosaki and Mikami, 2007; Kim et al., 2021). Changes in these atmospheric and land surface factors also shape the interannual and decadal variations in springtime dustiness across these two mid-latitude regions, ultimately affecting the regional human well-being.

Springtime dustiness across both East Asia and North America exhibits substantial interannual-to-decadal variations, with seemingly opposing trends across decades and divergent driving mechanisms reported by various studies (Kim et al., 2021; Kurosaki and Mikami, 2007; Xu et al., 2006). Based on satellite measurements of vegetation greenness and dust aerosol abundance, Wang et al. (2021) explained the decreased East Asian dustiness in spring by ecological restoration and resultant vegetation expansion for the period 2001-2020. In contrast, Wu et al. (2022) performed simulations with a dust emission model and identified surface wind speed weakening as the dominant driving mechanism for the decreased springtime dust emission across East Asia since 2000s. Apart from that, Song et al. (2021) regarded increasing vegetation and decreasing surface wind as main contributors of decreasing East Asian dust optical depth during 2009-2019. While this identified role of wind speed confirmed Tai et al. (2021)'s findings based on chemical transport model simulations, the latter study, covering the longer period since the 1980s, showed a different phase of decadal variations in East Asian dust emissions (Tai et al., 2021). Similar debates regarding the interannual-to-decadal variations in North American dustiness have also persisted. For example, statistical analysis with ground-based surface fine dust revealed warming and drying as the main cause of North American springtime dust emission's increase in the early 21st century (Achakulwisut et al., 2017). While according to ground-based dataset in the long-term, Pu and Ginoux (2018) attributed increased springtime surface fine dust concentrations to the decreasing trend in precipitation across Southwestern America for the period 1990-2015. Similar spatio-

https://doi.org/10.5194/egusphere-2025-4589
Preprint. Discussion started: 5 October 2025

temporal variation was interpreted by Hand et al. (2017) as a result of wind speed, soil moisture and land cover changes. In contrast, Pu and Ginoux (2017) studied satellite derived dust optical depth and established the primary relevance between land cover change and Southwestern North American springtime dust activities for the period 2004-2015. In the context of global warming, both regions' dust emissions appeared sensitive to vegetation expansion, according to global climate models and coupled dynamic vegetation-chemical transport model simulations (Li et al., 2021; Pu and Ginoux, 2017; Zong et al., 2021).

Despite the rich body of literature on the interannual to decadal variations in springtime mid-latitude dustiness, little consensus has emerged among these model- and observation-based studies regarding the direction of change and underlying mechanism. Observational datasets from ground- and satellite-based measurements provide estimates for atmospheric dust load in the past two to four decades but lack dust emission records. Therefore, the observed increase or decrease in atmospheric dust load could be sourced from both local and remote emissions, especially for the highly transportable mid-latitude dust (Yu et al., 2019b). On the other hand, dust emissions could be quantified using models, but the credibility of these models, especially their sensitivity to different influencing factors, should be validated against observation. Moreover, intense dust storm events that frequently occur in April-May are often modulated by cyclone activity. For instance, the extreme dust event over East Asia in March 2021 was attributed to both the increased intensity and frequency of Mongolian cyclones (Liang et al., 2022; Yin et al., 2022). Between 2001-2022, Mongolian cyclones were reported to contribute 34% to 47% of the total dust emissions from the Gobi Desert (Mu and Fiedler, 2025). However, quantitative analysis of how the characteristics of extratropical cyclones, including their occurrence, intensity and size, affect long-term variations in springtime dust activity across East Asia and North America remains lacking, which limits our understanding of the drivers behind dust's interannual to decadal variability.

This study aims to reconcile the interannual to decadal variations in dust emission across East Asia and North America and quantify the influence of multiple environmental factors. In this work, we simulate dust emissions across East Asia and North America in April and May from the late 20th century to the early 21st century using an observation-validated dust emission model and subsequently quantify the contribution of meteorology and land surface factors on dust emission

https://doi.org/10.5194/egusphere-2025-4589
Preprint. Discussion started: 5 October 2025

changes, including surface wind speed, soil moisture, snow cover fraction, surface temperature, leaf area index (LAI) from reanalysis and satellite-based observation datasets. Furthermore, this study integrates cyclone tracking and identification techniques to quantify the impact of extratropical cyclones on the interannual to decadal variations of both regions' dust activity over the past four decades. To clarify the reliability of the off-line dust emission model based on Ginoux et al. (2012), we compare the simulated changes in dust emission with ground-based and satellite-based dust measurements, such as the global dust Integrated Surface Database (duISD) during 1980-2019, the Interagency Monitoring of Protected Visual Environments (IMPROVE) network during 1988-2021 and the Moderate-resolution Imaging Spectroradiometer (MODIS) during 2000-2021.

2. Data and Method

2.1. Ground-based dust measurements

The observed extinction coefficient contributed by dust aerosol (β, km^{-1}) across East Asia (35 ° N-50° N, 90° E-120° E) is provided by global dust Integrated Surface Database (duISD) covering the period 1980-2019 (Xi, 2021). This dataset compiles about 30,000 stations globally, as collected by the National Oceanic and Atmospheric Administration (NOAA), and derives dust extinction coefficient from visibility observations as follows:

$$\beta = \frac{3.9}{V} \times f \,, \tag{1}$$

where β is a measure of the extinction coefficient caused by dust particles, V is the harmonic mean visibility, f is the dust frequency (%). 100 and 65 stations provide long-term observations across East Asia in April and May, respectively, with over two years' valid records during both the late 20th century (1980-1999) and the early 21st century (2000-2019).

Parallel to the duISD dataset, the Interagency Monitoring of Protected Visual Environments (IMPROVE) network has monitored the surface fine dust concentrations (μg m^{-3}) across North America (30° N-50° N, 103° W-118° W) since 1988. The IMPROVE network was originally designated to support the United States Environmental Protection Agency's Regional Haze Rule (Hand et al., 2019), and has subsequently been applied to air quality studies, including those on fine dust variations near the surface (Kim et al., 2021; Pu et al., 2022; Tong et al., 2017). The IMPROVE dataset provides individual species' contributions to $PM_{2.5}$ mass and total aerosol

https://doi.org/10.5194/egusphere-2025-4589
Preprint. Discussion started: 5 October 2025

extinction twice a week during 1988-2000 and every third day after 2000 in the United States (Pu et al., 2022). In this work we analyze the surface fine dust concentrations (μg m^{-3}) from 1988 to 2021 in April and May.

2.2. Satellite-based dust measurements

The Moderate-resolution Imaging Spectroradiometer (MODIS) with collection 6.1, level 1 provides the daily dust optical depth (DOD) during 2000-2021 at a spatial resolution of $0.1° \times 0.1°$. MODIS DOD is calculated from aerosol optical depth (AOD) and the Ångström exponent (α) as follows:

$$DOD = AOD \times (0.98 - 0.5089\alpha + 0.051\alpha^2), \quad (2)$$

The MODIS instrument is carried by both the Terra (equatorial overpassing at 10:30 a.m.) and Aqua (equatorial overpassing at 1:30 a.m.) satellites. DOD from MODIS is broadly used in the study of dust emission and atmospheric loading (Ginoux et al., 2012; Wu et al., 2022; Yu et al., 2019a; Yu and Ginoux, 2021, 2022).

2.3. Satellite-based vegetation measurements

The long-term global leaf area index (LAI) is provided by Global Inventory Modeling and Mapping Studies LAI product (GIMMS LAI4g) (Cao et al., 2023), with a half-month temporal resolution and a spatial resolution of 1/12° for the period 1982-2020. In this study, we expand the time range to 1980-2021 by replacing LAI in 1980-1981 with that in 1982 and LAI in 2021 with that in 2020. The GIMMS LAI4g product used the PKU GIMMS normalized difference vegetation index product (PKU GIMMS NDVI) and high-quality global Landsat LAI samples to remove the effects of satellite orbital drift and sensor degradation of Advanced Very High Resolution Radiometer (AVHRR). In the LAI model simulation, the MODIS Land Cover Type Product (MCD12Q1, version 6.1) provides the vegetation type reference.

2.4. Reanalysis data

To investigate the change in dust emissions and the contribution of several environmental variables in April and May, we analyze the 6-hourly snow cover fraction (%), top layer soil moisture (m^3 m^{-3}), land surface temperature (K) and hourly 10-m wind speed (m s^{-1}) from the European Centre for Medium-Range Weather Forecasts Reanalysis v5-Land (ERA5-LAND, referred to ERA5 hereafter)

https://doi.org/10.5194/egusphere-2025-4589
Preprint. Discussion started: 5 October 2025

during 1980-2021. The ERA5-LAND dataset is an enhanced global dataset produced by the European Centre for Medium-Range Weather Forecasts (ECMWF), with a native resolution of 9 km (Hersbach et al., 2020). The 10-m wind speed from ERA5 can capture the characteristics of wind to explore wind events both in the hourly and daily scales, compared with station observed wind speed from Hadley Centre's Integrated Surface Database (HadISD) (Molina et al., 2021).

2.5. Extratropical cyclone detection and tracking

To analyze regime shifts of extratropical cyclones (ECs) and their contribution to near-surface strong winds (> 6 m s^{-1}), we employed the Cyclone TRACKing framework (CyTRACK), an open-source Python toolbox for cyclone detection and tracking in reanalysis datasets (Pérez-Alarcón et al., 2024). CyTRACK identifies cyclone centers from mean sea level pressure (MSLP) fields at each time step and applies threshold-based filtering to track each cyclone. Previous evaluations have demonstrated that CyTRACK reliably reproduces interannual and seasonal variability, life-cycle characteristics, and spatial distributions of cyclone tracks when compared with ERA5-based best-track archives and other cyclone-track datasets.

In this work, we use the 6-hourly 10-m wind speed (m s^{-1}) and MSLP data in April and May from ERA5 to identify and track EC during 1980-2021, with a horizontal resolution of 0.25°. Cyclone centers are mainly identified based on two criteria: (1) surface relative vorticity exceeding 10^{-5} s^{-1}, a threshold widely applied in EC detection studies (Chen and Di Luca, 2025; Chen et al., 2022; Priestley et al., 2020), and (2) the central MSLP anomaly being at least 1 hPa lower than the surrounding grid points (Eichler and Higgins, 2006). Only cyclones with a lifetime longer than 24 hours are retained.

To quantify the contribution of ECs to strong winds and dust emissions across East Asia and North America, we determine whether hourly strong-wind events or dust emissions occurred within the spatial extent of each identified cyclone, defined by the cyclone size radius. The spatial extent of each cyclone is determined following Schenkel et al. (2017) as the radial distance from the cyclone center at which the azimuthal-mean 10-m wind speed equals a critical wind speed threshold. Following previous studies (Pérez-Alarcón et al., 2021; Pérez-Alarcón et al., 2024), we test several thresholds (2, 4, 6, 8, 10, and 12 m s^{-1}) and adopt 6 m s^{-1}, which both aligns with our definition of

https://doi.org/10.5194/egusphere-2025-4589
Preprint. Discussion started: 5 October 2025

strong winds and provides the most consistent results. All points within this radius are considered to be influenced by the cyclone.

2.6. Offline dust emission model

The quantification of historical, springtime dust emission change across East Asia and North America is achieved by an offline dust emission model, based on Ginoux et al. (2001) and Ginoux et al. (2012). Dust emission flux F_p is calculated as follows:

$$F_p = CSu_{max}^2(u_{max} - u_t), \quad (3)$$

In April and even occasionally in May, mid-to-high latitude dust source regions in East Asia and North America are partly covered by snow or frozen, which has a nonnegligible influence on dust emission (Balkanski et al., 2004; Yin et al., 2022). In this work, we take snow cover faction, surface temperature and vegetation cover into consideration, and define the simulated dust emission flux $F_{p-cover}$ with 0.1° × 0.1° spatial resolution as follows:

$$F_{p-cover} = F_p \times (1 - f_{snow}) \times \exp(-1 \times LAI) \times I, \quad (4)$$

where f_{snow} is daily snow cover fraction, LAI is daily vegetation cover and I is the indicator function of surface temperature (surface temperature > 0 ˚C, $I = 1$; surface temperature < 0 ˚C, $I = 0$). $C = 1.9$ μg s^2 m^{-5} is a dimensional factor, S is the fraction of dust source (Ginoux et al., 2010; Ginoux et al., 2012), approximated by the frequency of DOD > 0.2 for the period during 2000-2021 from MODIS in April and May, separately.

u_{max} is daily maximum surface wind speed in the original model and is substituted with hourly 10-m wind speed in the current study. u_t is the threshold wind velocity which is calculated as follows:

$$u_t = A \times u_{ref}\sqrt{\frac{\rho_p - \rho_a}{\rho_a} g \Phi_p}(1.2 + 0.2log_{10}w) \qquad (w < 0.5), \quad (5)$$

where $A = 6$ is a dimensionless parameter, u_{ref} is a reference threshold wind speed from Pu et al. (2020). ρ_a and ρ_p are the air and particle density, g is the gravitational acceleration, Φ_p is the particle diameter in five bins: 0.1-1 μm, 1-1.8 μm, 1.8-3.0 μm, 3.0-6.0 μm and 6.0-20.0 μm, according to (Kok et al., 2017), w is the top-layer soil moisture (m^3 m^{-3}).

2.7. Sensitivity experiments

https://doi.org/10.5194/egusphere-2025-4589
Preprint. Discussion started: 5 October 2025

To quantify the contribution of multiple environmental factors on East Asian and North American springtime dust emission changes, we conduct a set of sensitivity experiments that simulate controlled dust emissions. The controlled dust emissions are obtained by individually replacing the concurrent snow cover, temperature, soil moisture, hourly surface wind speed, and LAI during the controlled period with that during the baseline periods. These sensitivity experiments are conducted during the long (1980-2021) and short (2000-2021) terms as follows: in the long-term range, the time subsection is from the late 20th century (1980-2000, baseline period) to early 21st century (2001-2021, controlled period); in the short-term range, the time subsection is from 2000-2010 (baseline period) to 2011-2021 (controlled period) (Fig. 3). In this study, we use the percentage of dust emission changes between the controlled and baseline simulations to quantify the contribution of each meteorological and biological factor to the decadal changes in dust emission.

3. Results

3.1. Decadal variations in East Asian and North American dust emissions

Regional dust emission across East Asia mainly occurs in South Mongolia and North China, and has decreased insignificantly by 0.252 Tg month^{-1} decade^{-1} in April during the period 1980-2021 (Fig. 1a, c), as also captured by the reduction in dust extinction across the downwind region during 1980-2019 (Fig. 1c). The East Asian dust emission reduction in April is more pronounced after the onset of the 21st century, significantly (p-values < 0.05, based on the Mann-Kendall trend test) by 1.82 Tg month^{-1} decade^{-1} or 30.6% per two decades from 2000 to 2021 (Fig. 1a, e). Consistent with this simulated decrease in April dust emission, MODIS DOD exhibits a widespread, significantly (p-values < 0.05) negative trend in April of the early 21st century (Fig. 1a, e). Meanwhile, regional dust emission in North America shows a reversed multidecadal trend. North American dust emission has increased significantly (p-values < 0.05) by 0.261 Tg month^{-1} decade^{-1} or 30.1% per four decades in April during the period 1980-2021, confirmed by the surface fine dust concentrations during 1988-2021, especially in the lower latitudes (Fig. 2a, c). However, this increase is followed by a decrease in the regional total dust emissions by -0.388 Tg month^{-1} decade^{-1} or -13.3% per two decades in April for the period 2000-2021, consistently reflected by the satellite-based dust measurement (Fig. 2a, e).

https://doi.org/10.5194/egusphere-2025-4589
Preprint. Discussion started: 5 October 2025

247

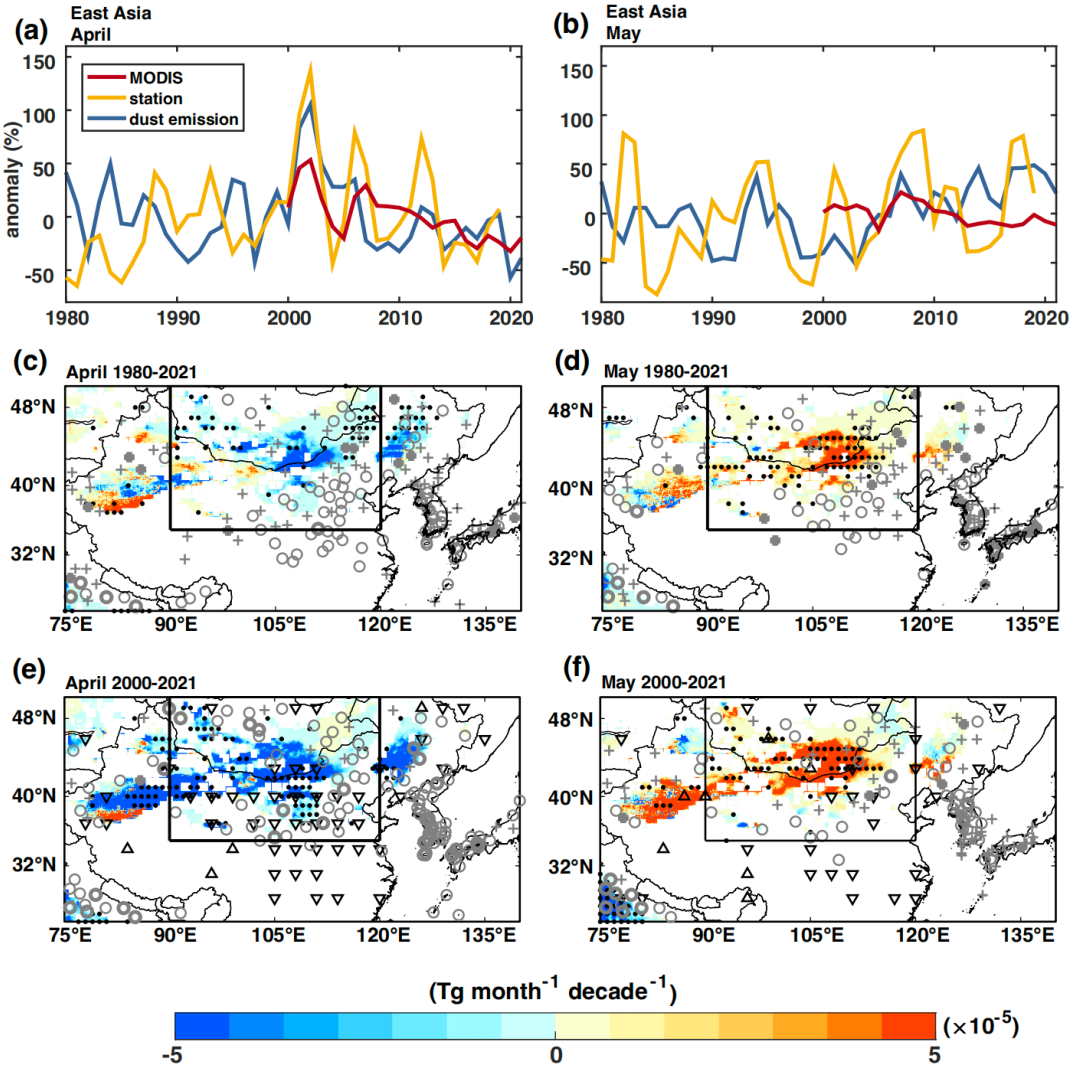

248

249 **Figure 1**. Changes of East Asian dustiness in April and May during 1980-2021 and 2000-2021.
250 Time series of DOD anomaly (red lines) from MODIS during 2000-2021, ground-observed
251 extinction coefficient contributed by dust aerosol anomaly (yellow lines) from duISD during 1980-
252 2019 and dust emissions anomaly (blue lines) from off-line simulation model during 1980-2021
253 across East Asia in (a) April and (b) May. Color shading represents the trend of simulated dust
254 emissions (Tg month^{-1} decade^{-1}) in (c, e) April and (d, f) May for the period (c, d) 1980-2021 and
255 (e, f) 2000-2021. Stippled areas exhibit statistically significant dust emission trends (p-values <

https://doi.org/10.5194/egusphere-2025-4589
Preprint. Discussion started: 5 October 2025

0.1, based on the Mann-Kendall trend test). Grey pluses and hollow circles indicate positive and negative, respectively, trends in columnar dust amount during (c, d) 1980-2019 and (e, f) 2000-2019 from duISD. Bold pluses and hollow circles indicate significant (p-values < 0.1, based on the Student's t-test) trends in the corresponding dustiness observation. In (e, f), bold black upward- and downward-pointing triangles indicate significant (p-values < 0.1, based on the Mann-Kendall trend test) positive and negative trends in DOD from MODIS in 2000-2021. Boxes denote studied dust source regions across East Asia.

In contrast, both East Asian and North American dust emissions show a steady increase in May during the past four decades. The regional total dust emission is estimated to have increased significantly (p-values < 0.05) by 0.321 and 1.05 Tg month^{-1} decade^{-1} or 28.8% and 36.7% across East Asia in May for the period 1980-2021 and 2000-2021 (Fig. 1b, d, f). The duISD and MODIS datasets indicates a significant (p-values < 0.1) dust increment across South Mongolia and North China in May for the period 1980-2019 and 2000-2021, respectively (Fig. 1b, d). In North America, the regional total dust emission has increased by 0.226 and 0.171 Tg month^{-1} decade^{-1} or 20.0% and 15.5% in May during 1980-2021 and 2000-2021 (Fig. 2b, d, f), respectively, consistent with the ground- and satellite-based dustiness observations. Additionally, North American dust emission in May shows a latitudinal variation, with a decrease in dust emissions at higher latitudes and an increase at lower latitudes, particularly in the early 21st century (2000-2021) (Fig. 2f).

https://doi.org/10.5194/egusphere-2025-4589
Preprint. Discussion started: 5 October 2025

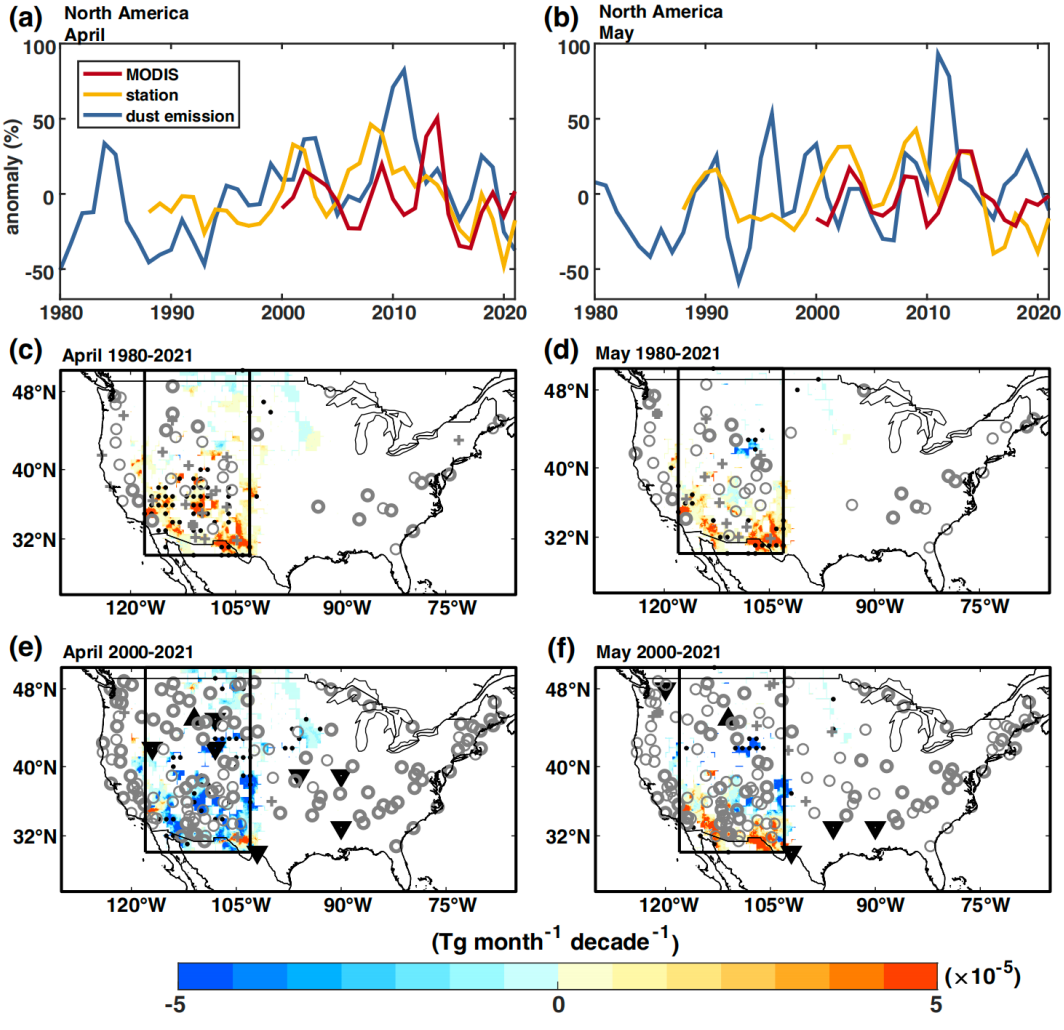

Figure 2. Changes of North American dustiness in April and May during 1980-2021 and 2000-2021. Time series of DOD anomaly (red lines) from MODIS during 2000-2021, ground-observed extinction coefficient contributed by dust aerosol anomaly (yellow lines) from IMPROVE during 1988-2021 and dust emissions anomaly (blue lines) from off-line simulation model during 1980-2021 across North America in (a) April and (b) May. Color shading represents the trend of simulated dust emissions (Tg month^{-1} decade^{-1}) in (c, e) April and (d, f) May for the period (c, d) 1980-2021 and (e, f) 2000-2021. Stippled areas exhibit statistically significant dust emission trends (p-values < 0.1, based on the Mann-Kendall trend test). Grey pluses and hollow circles indicate positive and negative, respectively, trends in columnar dust amount during (c, d) 1988-2021 and

https://doi.org/10.5194/egusphere-2025-4589
Preprint. Discussion started: 5 October 2025

(e, f) 2000-2021 from IMPROVE. Bold pluses and hollow circles indicate significant (p-values < 0.1, based on the Student's t-test) trends in the corresponding dustiness observation. In (e, f), bold black upward- and downward-pointing triangles indicate significant (p-values < 0.1, based on the Mann-Kendall trend test) positive and negative trends in DOD from MODIS in 2000-2021. Boxes denote studied dust source regions across North America.

3.2. Influencing factors of dust emission changes since the 1980s

The contributions of several environmental variables to the decadal variations in regional dust emissions are disentangled by the sensitivity experiments. The multidecadal change in East Asian dust emission in April during 1980-2021 has been mainly driven by soil moisture decrease and surface warming with reduced snow cover, which individually causes a 3.55% and 2.59% increase in dust emission (Fig. 3b). Except for this leading role of soil moisture and temperature in dust emission's multidecadal variation in April across East Asia, surface wind speed emerges as the main driver of dust emission variations in April and May across both East Asia and North America (Fig. 3c, e, f, Fig. 4). For example, during 1980-2021, the changes in surface wind speed have made a positive contribution to dust emission increase by 0.802% and 32.3% across East Asia and North America, respectively, in April (Fig. 3b, 4b), and a corresponding regional contribution of 26.8% and 13.3% in May (Fig. 3e, 4e). During 2000 to 2021, the surface wind speed has caused a reduction in dust emissions by -34.8% and -11.3% across East Asia and North America in April (Fig. 3c, 4c) and an increment by 38.3% and 16.5% in May (Fig. 3f, 4f). On the contrary, changes in vegetation contribute minimally to dust emission changes over East Asia and North America during the same periods (Fig. 3, 4), likely due to lack of significant, positive trends in LAI across both regions in both April and May, especially in the longer term (Fig. 5).

https://doi.org/10.5194/egusphere-2025-4589
Preprint. Discussion started: 5 October 2025

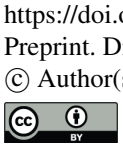

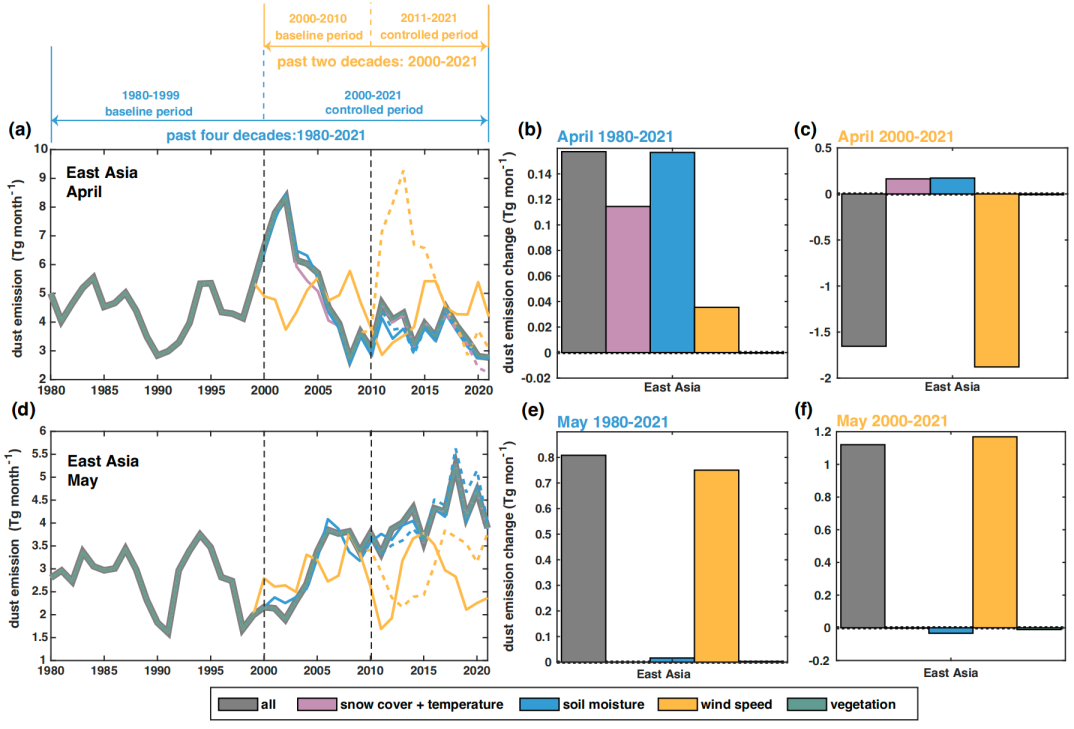

Figure 3. Changes in East Asian dust emission (Tg month^{-1}) and the contribution of several environmental variables during 1980-2021. Time series of total dust emission (grey) and controlled dust emission in the sensitivity experiments (colored) across East Asia in (a-c) April and (d-f) May. The solid, colored lines during 2001-2021 reflect the dust emissions if each environmental variable repeats their values during 1980-2000; the dashed, colored lines during 2011-2021 reflect the dust emissions if each environmental variable repeats their values during 2000-2010. (b, c, e, f) Dust emission change (Tg month^{-1}) and the contribution of each factor (color-coded the same way as in a, d) across East Asia in (b, c) April and (e, f) May in past four decades (blue font and lines in the upper of subplot a) and past two decades (yellow font and lines in the upper of subplot a).

https://doi.org/10.5194/egusphere-2025-4589
Preprint. Discussion started: 5 October 2025

322

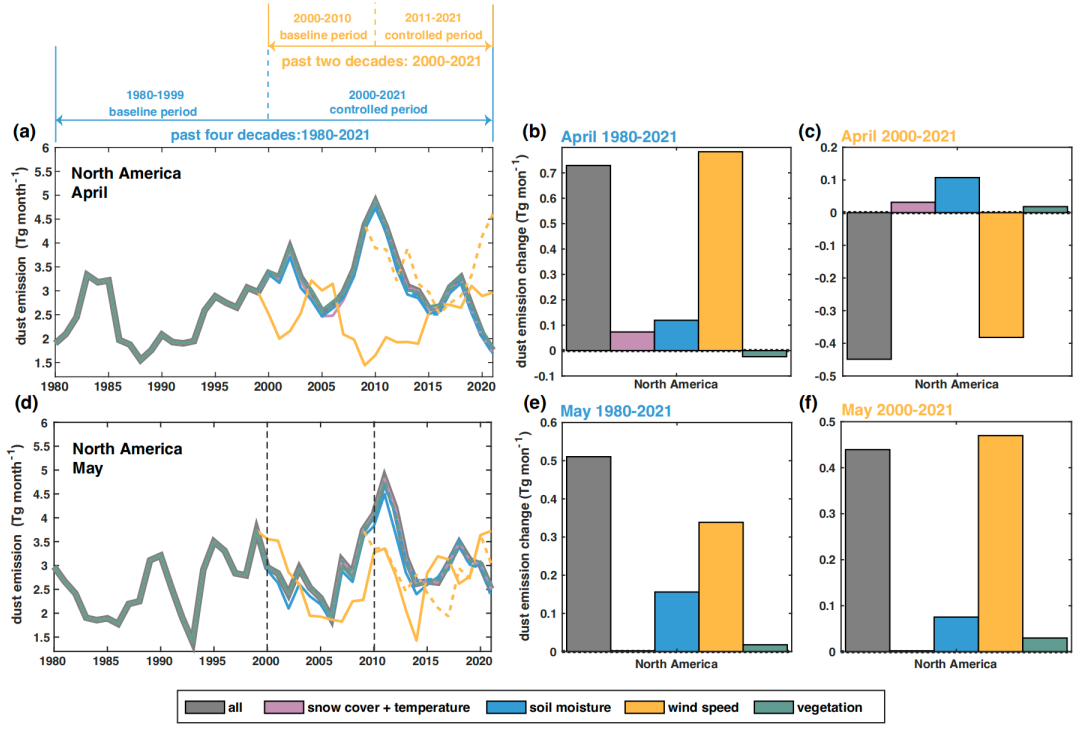

323

324 **Figure 4**. Changes in North American dust emission (Tg month^{-1}) and the contribution of several
325 environmental variables during 1980-2021. Figure elements are identical to those in Fig. 3.

https://doi.org/10.5194/egusphere-2025-4589
Preprint. Discussion started: 5 October 2025

326

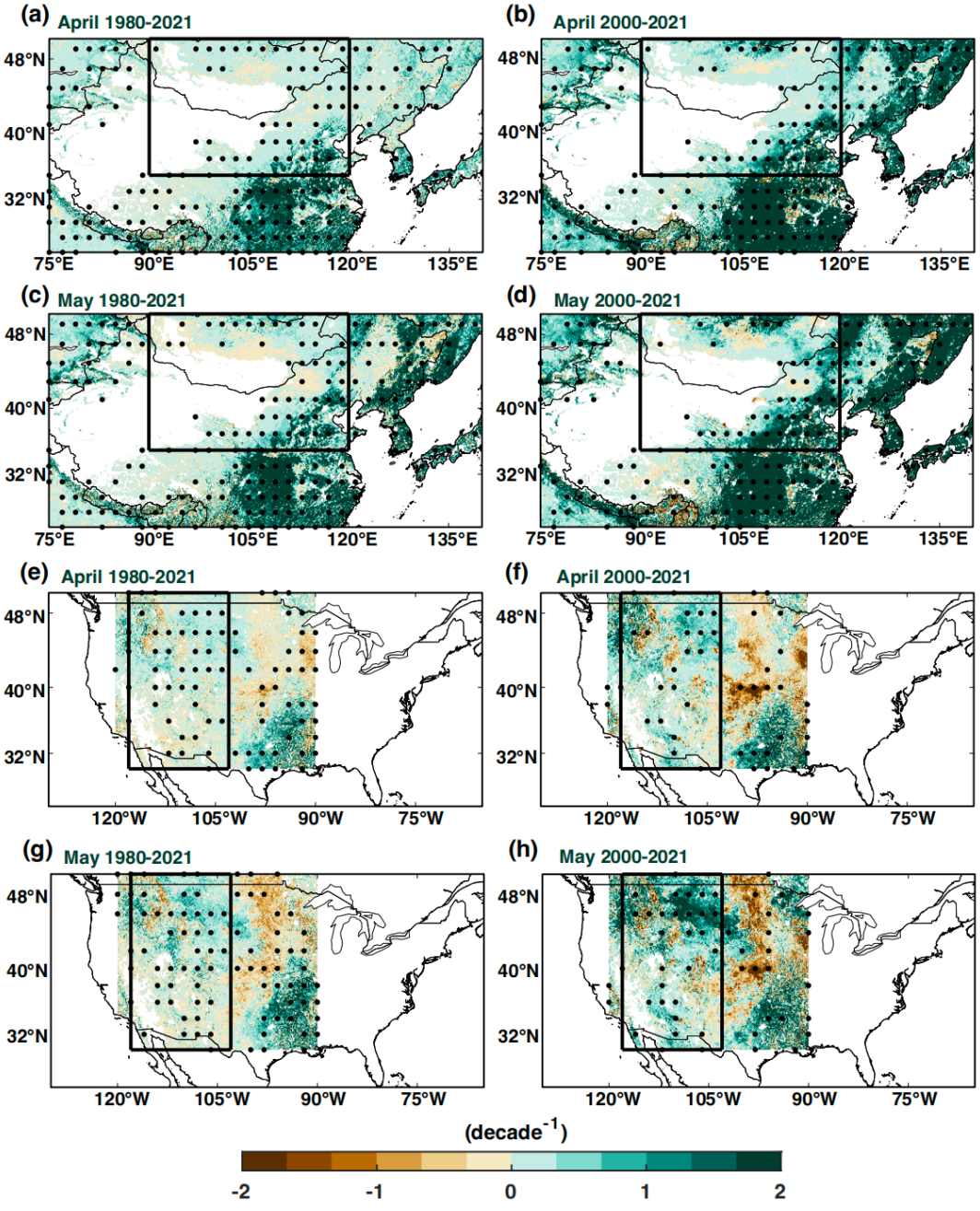

327

328 **Figure 5. Changes of LAI in April and May for the period 1980-2021 and 2000-2021.** Trends
329 in (a, b) April and (c, d) May LAI (decade^{-1}) across East Asia for the period (a, c) 1980-2021 and

https://doi.org/10.5194/egusphere-2025-4589
Preprint. Discussion started: 5 October 2025

(b, d) 2000-2021.Trends in (e, f) April and (g, h) May daily LAI (decade^{-1}) across North America for the period (e, g) 1980-2021 and (f, h) 2000-2021, respectively. Black dots indicate significant (p-values < 0.1, based on the Mann-Kendall trend test) trend in LAI from GIMMS.

3.3 Changing frequency and duration of strong winds

As the dominant influencing factor of East Asian and North American dust emission in mid-to-late spring, near-surface wind speed shows spatio-temporally in-phase variations with dust emission. Spatially, daily maximum wind speed (Fig. 6) exhibits similar patterns of change with those in dust emissions across both regions during both the shorter and longer periods (Fig. 1, 2). Temporally, the positive contribution of wind speed to dust emission across North America in April during 1980-2021 (Fig. 4b) and across both regions in May during the entire period 1980-2021 (Fig. 3e, f, 4e, f) is a consequence of the higher occurrence of longer-lasting strong winds (Fig. 7). For example, the occurrence of strong winds with duration between 150 and 260 hours and frequency between 18 and 34 events per month has increased significantly across North America in April (Fig. 7h), leading to the positive trend of daily maximum wind speed across North America in April from the late 20th century (1980-2000) to the early 21st century (2001-2021) (Fig. 4). Similarly, strong winds that last for over 150 hours, typically associated with synoptic weather systems, occur more frequently in May across both regions during the recent decades (Fig. 7), resulting in the multidecadal, steady increase in dust emission from both regions in May (Fig. 1, 2, 4).

https://doi.org/10.5194/egusphere-2025-4589
Preprint. Discussion started: 5 October 2025

352

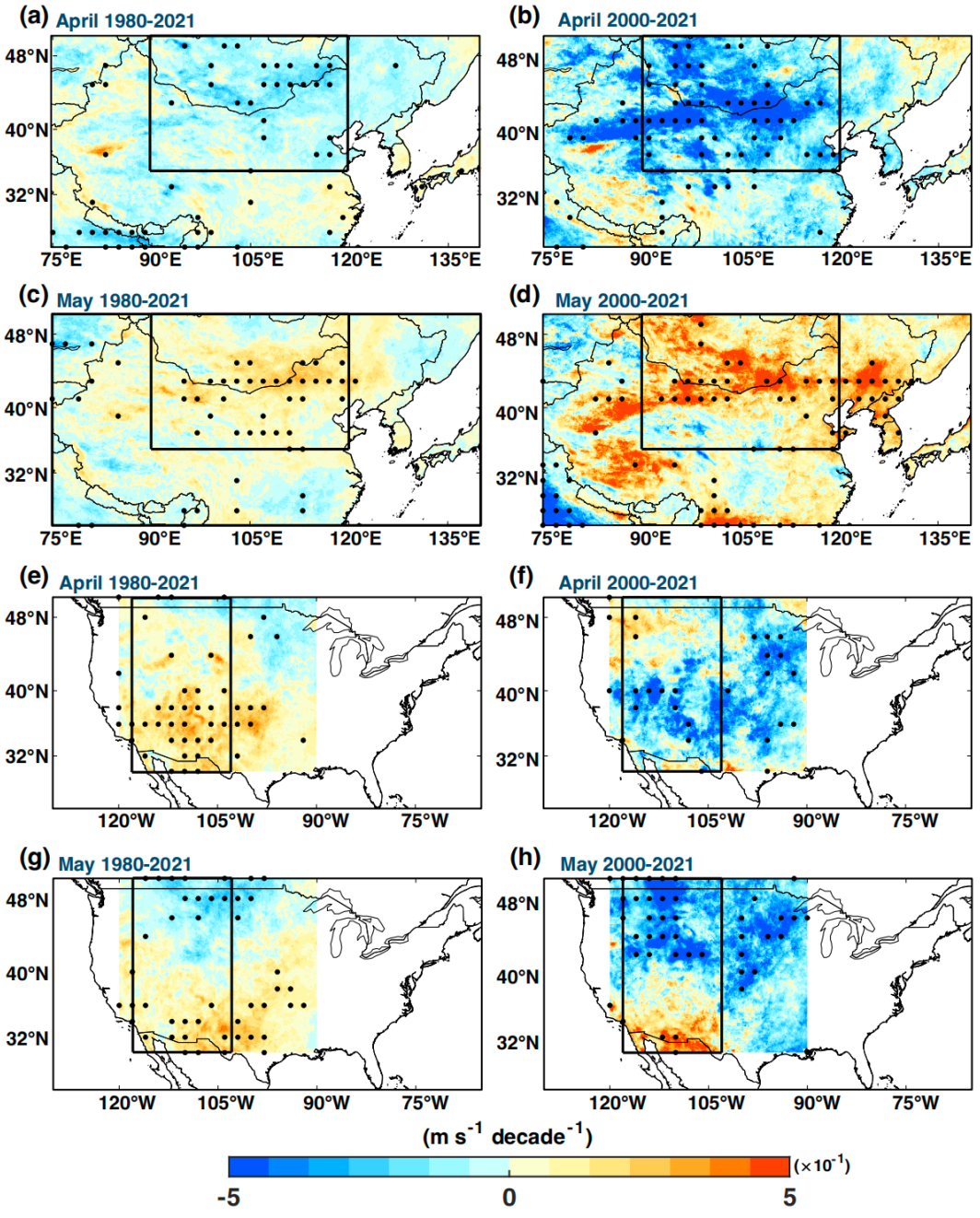

353

354 **Figure 6. Changes of daily maximum wind speed in April and May for the period 1980-2021**
355 **and 2000-2021.** Trends in (a, b) April and (c, d) May daily maximum wind speed (m s^{-1} $decade^{-1}$)

https://doi.org/10.5194/egusphere-2025-4589
Preprint. Discussion started: 5 October 2025

356 across East Asia for the period (a, c) 1980-2021 and (b, d) 2000-2021.Trends in (e, f) April and (g,
357 h) May daily maximum wind speed (m s^{-1} $decade^{-1}$) across North America for the period (e, g)
358 1980-2021 and (f, h) 2000-2021, respectively. Black dots indicate significant (*p*-values < 0.1,
359 based on the Mann-Kendall trend test) trend in daily maximum wind speed.
360

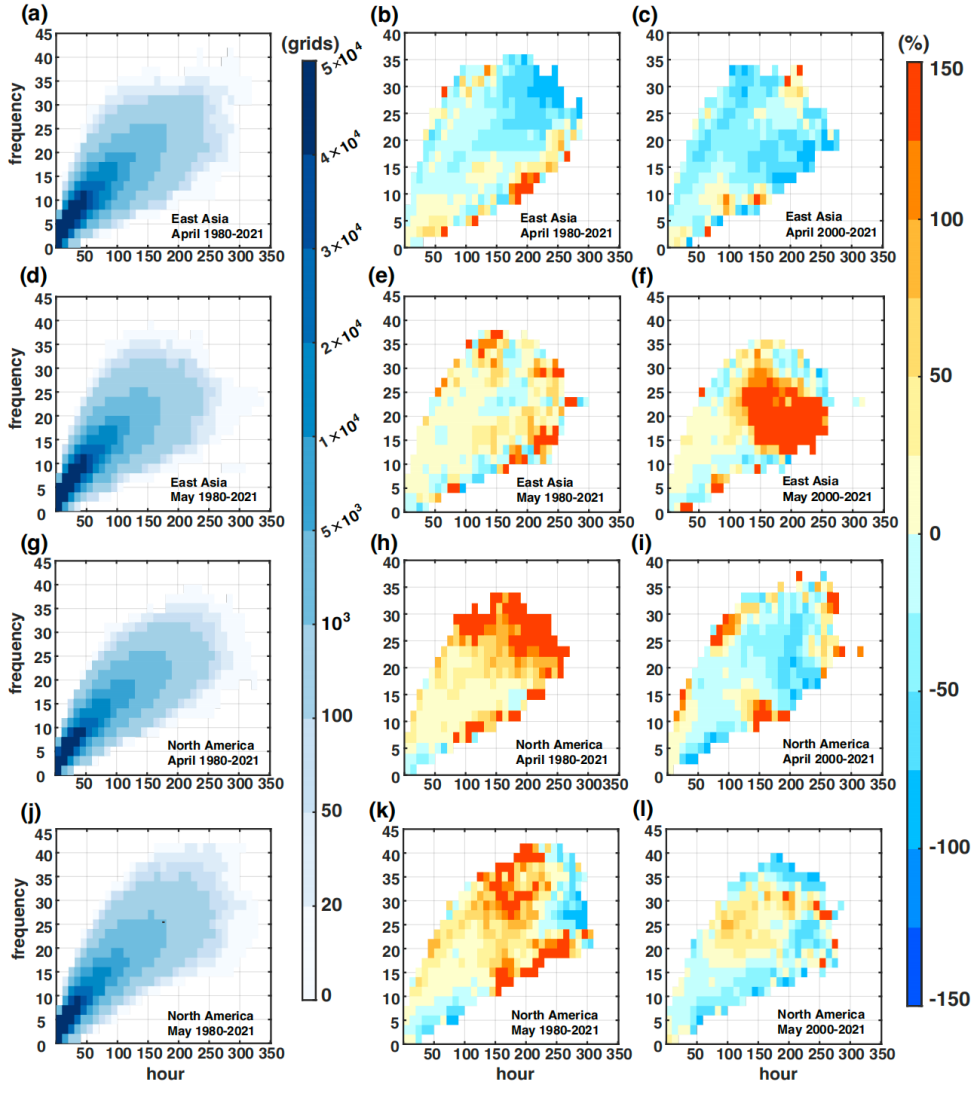

361

362 **Figure 7. Changes of strong wind across East Asia and North America in April and May.**
363 Joint probability distribution (joint PDF) of the monthly total frequency and duration of strong
364 wind (> 6 m s^{-1}) from ERA5 hourly 10-m wind speed data across the dust-emitting pixels in (a, d)

https://doi.org/10.5194/egusphere-2025-4589
Preprint. Discussion started: 5 October 2025

East Asia and (g, j) in North America in (a, g) April and (d, j) May during 1980-2021. Change rate (%) of the joint PDF of the frequency (events per month) and duration (hours per month) of strong winds (> 6 m s^{-1}) to baseline periods from ERA5 hourly 10-m wind speed data across the dust-emitting pixels in (b, c, e, f) East Asia in (b, c) April and (e, f) May for the period (b, e) 1980-2021, (c, f) 2000-2021 and in (h, i, k, l) North America in (h, i) April and (k, l) May for the period (h, k) 1980-2021, (i, l) 2000-2021.

3.4 Regime shifts of extratropical cyclones

Extratropical cyclones exert a significant influence on near-surface strong winds during April and May, which in turn affect dust emission processes. In East Asia, the annual average occurrence and maximum wind speed (Vmax) of extratropical cyclone, duration of cyclone-driven strong winds, and cyclone-induced dust emissions showed no substantial changes in April from 1980 to 2021 (Fig. 8a, 9a). However, all four factors exhibited distinct inter-decadal variability during 2000-2021 (Fig. 8a, 9a). This pattern aligns with the currently identified, minimal overall contribution of wind to dust emission changes in East Asia in April from 1980 to 2021 (Fig. 3a, b, 7b), and explains the decline in dust emissions associated with reduced strong winds from 2000 to 2021 (Fig. 3a, c, 7c). In May, the increase in both the duration of strong winds and cyclone frequency shaped the frequency and duration of strong winds' change pattern in East Asia between 1980-2021 and 2000-2021 (Fig. 7e, f, 8b), thereby driving the inter-decadal variability in dust emissions (Fig. 3d, e, f, 9b).

The increased North American dust emissions in April from 1980 to 2021, driven by longer-lasting and more frequent strong winds (Fig. 4b, 7h), also can be attributed to changes in extratropical cyclones. During this period, both the number of extratropical cyclones and their maximum wind speed increased, resulting in longer durations of strong winds (Fig. 8c). In contrast, from 2000 to 2021, the decrease in the number of cyclones and Vmax, along with shorter periods of cyclone-caused strong winds, leads to the decline in wind-driven dust emissions in April, which dominate the inter-decadal variability of dust emissions (Fig. 4c, 7i, 8c, 9c). In May, the changes in strong winds during 1980-2021 can also be explained by variations in extratropical cyclones and their associated strong wind durations. More frequent and stronger cyclones cause extended periods of strong winds, leading to higher North American dust emissions (Fig. 4e, 7k, 8d, 9d). However, for

https://doi.org/10.5194/egusphere-2025-4589
Preprint. Discussion started: 5 October 2025

the period in 2000-2021, although the duration of cyclone-caused strong winds increases slightly (Fig. 8d), the percentage of dust emissions driven by extratropical cyclones have weakened (Fig. 9d). This may be explained by the reduced number and radius of cyclones (Fig. 8d), which lead to a relative decrease in the area affected by cyclone-induced dust activity; meanwhile, within the cyclone-affected regions, stronger winds enhanced dust emission intensity. During the period in 2000-2021, cyclone-induced dust emissions remain nearly constant, whereas dust emissions from non-cyclone strong wind events increased (Fig. 9d), likely due to enhanced smaller-scale or weaker-magnitude disturbances.

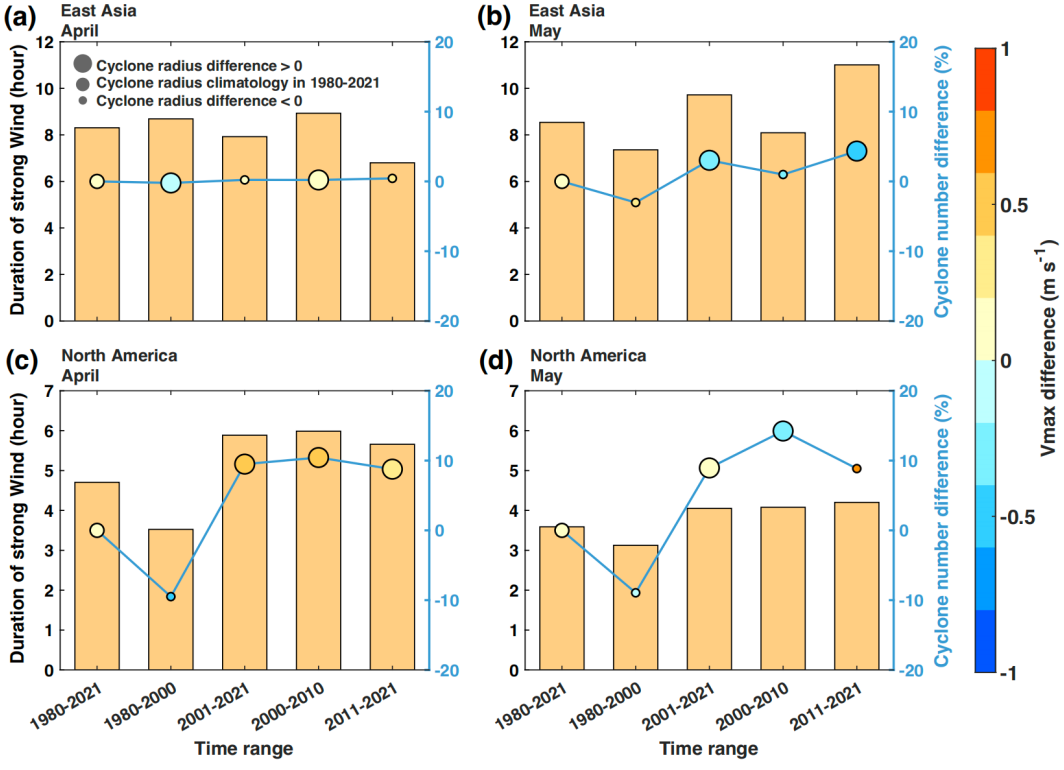

Figure 8. Regime shifts in extratropical cyclones across East Asia and North America during April and May across different time periods from 1980 to 2021. The monthly average duration of strong winds (hours; yellow bars) caused by extratropical cyclones in (a, b) East Asia and (c, d) North America in (a, c) April and (b, d) May, for the time periods: 1980-2021, 1980-2000, 2001-2021, 2000-2010, and 2011-2021, with reference to the left y-axis. The blue solid line with markers

https://doi.org/10.5194/egusphere-2025-4589
Preprint. Discussion started: 5 October 2025

411 represents the difference in the monthly average number of cyclones during these periods
412 compared to the monthly average cyclone count during the whole period 1980-2021,
413 corresponding to the right blue y-axis. Marker color shows the deviation of monthly mean Vmax
414 (m s^{-1}) from the 1980-2021 climatology, and marker size reflects the cyclone radius difference
415 relative to the 1980-2021 mean.
416

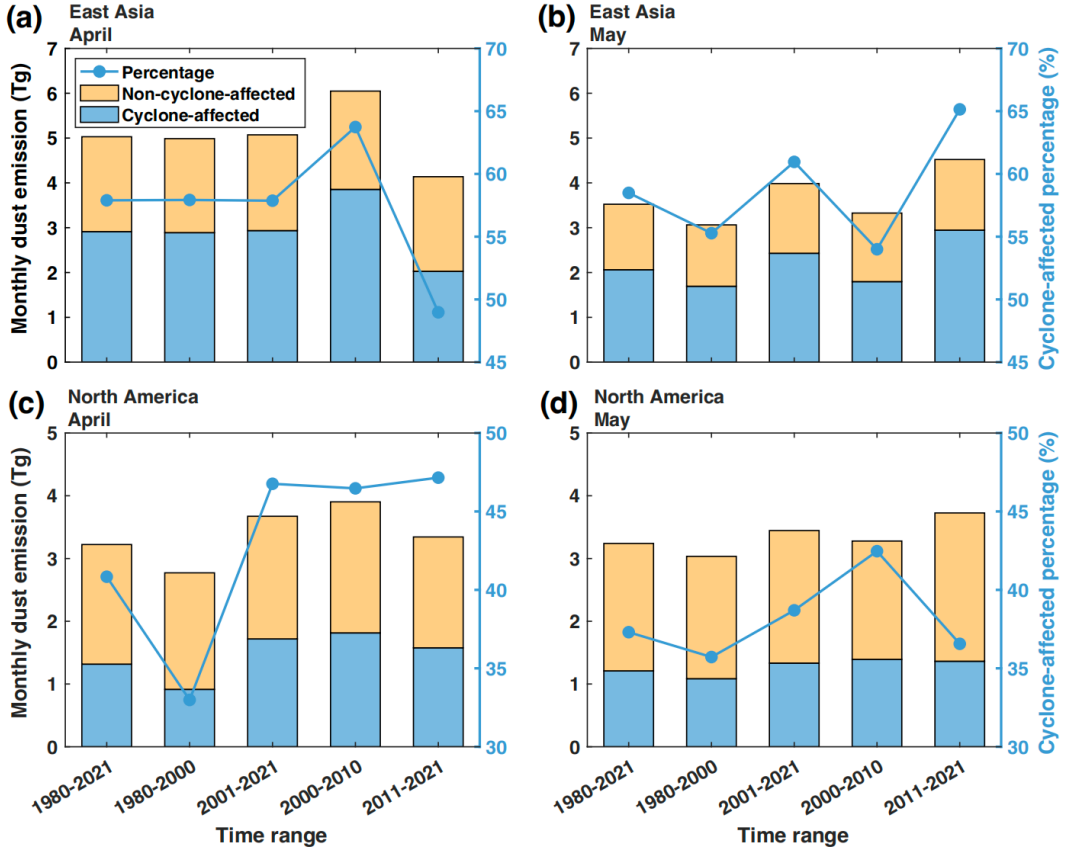

417

418 **Figure 9.** Regime shifts in extratropical cyclone-caused dust emissions (Tg) across East Asia and
419 North America in April and May across different time periods from 1980 to 2021. The annual
420 average dust emissions (Tg) along the passage of extratropical cyclones (blue bars) and those
421 unaffected by them (yellow bars) are shown for (a, b) East Asia and (c, d) North America in (a, c)
422 April and (b, d) May, for the time periods: 1980-2021, 1980-2000, 2001-2021, 2000-2010, and
423 2011-2021, with reference to the left y-axis. The blue solid line represents the percentage of dust

https://doi.org/10.5194/egusphere-2025-4589
Preprint. Discussion started: 5 October 2025

emissions affected by extratropical cyclones (%) over these periods, corresponding to the right y-axis.

4. Discussion and conclusion

Based on a suite of multi-source observational datasets and a dust emission model, we characterize the decadal variability of mid-to-late springtime dust emissions across East Asia and North America, which are primarily regulated by changes in surface wind speed and extratropical cyclone activity during the recent decades. During the past four decades, the East Asian and North American drylands exhibit a 4% and 30% increase in April dust emissions and a 29% and 20% increase in May. During the past two decades, these two regions show a 31% and 13% decrease in April dust emissions and a 37% and 16% increase in May. Our results highlight the dominant role of surface wind speed in shaping decadal variations of dust emissions, while the frequency and intensity of extratropical cyclones exert substantial influence on wind speed variability. Collectively, these two factors constitute the primary drivers of regional total dust emission changes across East Asia and North America in the late 20th century and early 21st century. Overall, our study provides a clearer understanding of the decadal-scale variability of mid-to-late springtime dust emissions across East Asia and North America, and underscores the primary roles of both surface wind speed and extratropical cyclones in modulating dust emission changes.

In this study, we demonstrate the leading influence of surface wind speed on decadal changes of dust emission. Wind speed regimes, especially the frequency, duration, and intensity of strong wind events, reflect the signal of both climate variability and climate change. Extratropical cyclones exert a dominant influence on near-surface strong winds, which in turn drive dust emissions. The identified decadal changes in near-surface wind speed, along with the changing duration of strong wind events, can be largely attributed to regime shifts in extratropical cyclones (Fig. 7, 8, 9). In addition, these changes may also be interpreted as part of (1) the response in mid-latitude storm track processes to global warming (Shaw et al., 2016), (2) regional climate oscillations associated with large scale modes of climate oscillation, such as El Niño-Southern Oscillation (ENSO), North Atlantic Oscillation (NAO), Pacific Decadal Oscillation (PDO), Arctic Oscillation (AO) etc. (Yin et al., 2022), and (3) global surface wind stilling up to 2010 and subsequent recovery attributed to internal climate variability (Zeng et al., 2019; Wohland et al., 2021).

https://doi.org/10.5194/egusphere-2025-4589
Preprint. Discussion started: 5 October 2025

Compared with wind speed, land surface changes seem secondary in shaping the decadal variations in dust emission, except the slight dust emission increase across East Asia in April since the 1980s in response to surface warming, reduced snow cover, and soil moisture. Beyond reflecting the mixed signals from climate variability, land surface factors directly respond to climate change. For example, studies on vegetation phenology have reported an earlier greening trend across Northern Hemispheric mid-latitudes in response to early-spring warming and CO_2 fertilization (Fan et al., 2014; Piao et al., 2019). But vegetation's increasingly stronger inhibition on dust emission appears unable to offset the influence of surface wind speed for the period 1980-2021 (Fig. 5). Furthermore, future changes in vegetation cover highly depend on the competing trajectories of surface temperature and soil moisture, and their role in dust emission remains uncertain (Ding et al., 2020).

The uncertainty of our study mainly comes from the limitation of observational datasets and dust emission model. First, station observations generally lack temporal continuity and spatial coverage especially in dust source regions; therefore, the long-term trend in dustiness from stations likely miss the complete spatio-temporal pattern. Second, higher albedo of cloud and land surface, in the presence of thick clouds and snow, respectively, brings challenge to satellite aerosol retrieval algorithms, preventing a more accurate quantification of dust concentration or emission solely based on satellite data. Third, although the simulation from off-line dust emission model generally matches observed spatio-temporal variations, this parameterization inevitably underrepresents actual physical processes, similar to all dust emission models currently being used, especially the interaction between environmental variables. For example, we estimate the area of unvegetated, wind-erosive regions within each grid by $\exp(-1 \times LAI)$ (Pu and Ginoux, 2017). This parameterization, however, omits the influence of vegetation height and canopy structure on near-surface wind profile and eventually the frictional wind speed that is directly responsible for dust emission. This uncertainty in dust emission modeling will be quantified and reduced upon an expanded collection of observable data, e.g. meter-resolution vegetation structure, spatio-temporally resolved near-surface wind speed profiles, in conjunction with satellite measurement of dust aerosol abundance with finer spatio-temporal resolutions.

Data Availability Statement

https://doi.org/10.5194/egusphere-2025-4589
Preprint. Discussion started: 5 October 2025

Data used in this study are all publicly available, including: the MODIS Deep Blue aerosol products acquired from the Level-1 and Atmosphere Archive and Distribution System (LAADS) Distributed Active Archive Center (DAAC) (https://doi.org/10.5194/amt-6-949-2013); the ERA-5 hourly climate data provided by European Centre for Medium-Range Weather Forecasts (ECMWF) (https://doi.org/10.5194/essd-13-4349-2021); the GIMMS leaf area index at a half-month temporal resolution acquired from Cao et al. (2023); the global dust Integrated Surface Database (duISD) acquired from Xi (2021); the Interagency Monitoring of Protected Visual Environments (IMPROVE) network is available for download (http://vista.cira.colostate.edu/improve).

Code Availability

The code to carry out the current analyses is available from the corresponding authors upon request.

Acknowledgments

This research is supported by Beijing Natural Science Foundation grant JQ23037 (J.N.) and NSFC grant number 42275016 (Y.Y.). We thank Paul Ginoux for useful discussions. Computation is supported by High-performance Computing Platform of Peking University.

Author contributions

YY conceived the study. YW and YY performed the analysis and wrote the initial draft. All authors contributed to the data analysis and manuscript editing.

Competing interests

The authors declare that they have no conflict of interest.

References

Achakulwisut, P., Shen, L., and Mickley, L. J.: What Controls Springtime Fine Dust Variability in the Western United States? Investigating the 2002-2015 Increase in Fine Dust in the U.S. Southwest, Journal of Geophysical Research: Atmospheres, 122, 12449-12467, https://doi.org/10.1002/2017jd027208, 2017.

Adebiyi, A., Kok, J. F., Murray, B. J., Ryder, C. L., Stuut, J.-B. W., Kahn, R. A., Knippertz, P., Formenti, P., Mahowald, N. M., Pérez García-Pando, C., Klose, M., Ansmann, A., Samset, B. H., Ito, A., Balkanski, Y., Di Biagio, C., Romanias, M. N., Huang, Y., and Meng, J.: A review of coarse mineral dust in the Earth system, Aeolian Research, 60, 100849, https://doi.org/10.1016/j.aeolia.2022.100849, 2023.

https://doi.org/10.5194/egusphere-2025-4589
Preprint. Discussion started: 5 October 2025

Aryal, Y. and Evans, S.: Decreasing Trends in the Western US Dust Intensity With Rareness of Heavy Dust Events, Journal of Geophysical Research: Atmospheres, 127, e2021JD036163, https://doi.org/10.1029/2021jd036163, 2022.

Balkanski, Y., Schulz, M., Claquin, T., Moulin, C., and Ginoux, P.: Global Emissions of Mineral Aerosol: Formulation and Validation using Satellite Imagery. In: Granier, C., Artaxo, P., Reeves, C.E. (eds) Emissions of Atmospheric Trace Compounds, Advances in Global Change Research, 18, 2004.

Cao, S., Li, M., Zhu, Z., Wang, Z., Zha, J., Zhao, W., Duanmu, Z., Chen, J., Zheng, Y., Chen, Y., Myneni, R. B., and Piao, S.: Spatiotemporally consistent global dataset of the GIMMS leaf area index (GIMMS LAI4g) from 1982 to 2020, Earth System Science Data, 15, 4877-4899, https://doi.org/10.5194/essd-15-4877-2023, 2023.

Chen, S., Huang, J., Zhao, C., Qian, Y., Leung, L. R., and Yang, B.: Modeling the transport and radiative forcing of Taklimakan dust over the Tibetan Plateau: A case study in the summer of 2006, Journal of Geophysical Research: Atmospheres, 118, 797-812, https://doi.org/10.1002/jgrd.50122, 2013.

Chen, T. C. and Di Luca, A.: Characteristics of Precipitation and Wind Extremes Induced by Extratropical Cyclones in Northeastern North America, Journal of Geophysical Research: Atmospheres, 130, https://doi.org/10.1029/2024jd042079, 2025.

Chen, T. C., Di Luca, A., Winger, K., Laprise, R., and Thériault, J. M.: Seasonality of Continental Extratropical-Cyclone Wind Speeds Over Northeastern North America, Geophysical Research Letters, 49, https://doi.org/10.1029/2022gl098776, 2022.

Ding, Y., Li, Z., and Peng, S.: Global analysis of time-lag and -accumulation effects of climate on vegetation growth, International Journal of Applied Earth Observation and Geoinformation, 92, 102179, https://doi.org/10.1016/j.jag.2020.102179, 2020.

Eichler, T. and Higgins, W.: Climatology and ENSO-Related Variability of North American Extratropical Cyclone Activity, Journal of Climate, 19, 2076-2093, https://doi.org/https://doi.org/10.1175/JCLI3725.1, 2006.

Fan, B., Guo, L., Li, N., Chen, J., Lin, H., Zhang, X., Shen, M., Rao, Y., Wang, C., and Ma, L.: Earlier vegetation green-up has reduced spring dust storms, Scientific Reports, 4, 6749, https://doi.org/10.1038/srep06749, 2014.

Ginoux, P., Garbuzov, D., and Hsu, N. C.: Identification of anthropogenic and natural dust sources using Moderate Resolution Imaging Spectroradiometer (MODIS) Deep Blue level 2 data, Journal of Geophysical Research, 115, D05204, https://doi.org/10.1029/2009jd012398, 2010.

Ginoux, P., Prospero, J. M., Gill, T. E., Hsu, N. C., and Zhao, M.: Global-scale attribution of anthropogenic and natural dust sources and their emission rates based on MODIS Deep Blue aerosol products, Reviews of Geophysics, 50, 3, https://doi.org/10.1029/2012rg000388, 2012.

Ginoux, P., Chin, M., Tegen, I., Prospero, J. M., Holben, B., Dubovik, O., and Lin, S.-J.: Sources and distributions of dust aerosols simulated with the GOCART model, Journal of Geophysical Research: Atmospheres, 106, 20255-20273, https://doi.org/10.1029/2000jd000053, 2001.

Gui, K., Yao, W., Che, H., An, L., Zheng, Y., Li, L., Zhao, H., Zhang, L., Zhong, J., Wang, Y., and Zhang, X.: Record-breaking dust loading during two mega dust storm events over northern China in March 2021: aerosol optical and radiative properties and meteorological

https://doi.org/10.5194/egusphere-2025-4589
Preprint. Discussion started: 5 October 2025

drivers, Atmospheric Chemistry and Physics, 22, 7905-7932, https://doi.org/10.5194/acp-22-7905-2022, 2022.
Hand, J. L., Gill, T. E., and Schichtel, B. A.: Spatial and seasonal variability in fine mineral dust and coarse aerosol mass at remote sites across the United States, Journal of Geophysical Research: Atmospheres, 122, 3080-3097, https://doi.org/10.1002/2016jd026290, 2017.
Hand, J. L., Prenni, A. J., Schichtel, B. A., Malm, W. C., and Chow, J. C.: Trends in remote PM2.5 residual mass across the United States: Implications for aerosol mass reconstruction in the IMPROVE network, Atmospheric Environment, 203, 141-152, https://doi.org/10.1016/j.atmosenv.2019.01.049, 2019.
Hashizume, M., Kim, Y., Ng, C. F. S., Chung, Y., Madaniyazi, L., Bell, M. L., Guo, Y. L., Kan, H., Honda, Y., Yi, S. M., Kim, H., and Nishiwaki, Y.: Health Effects of Asian Dust: A Systematic Review and Meta-Analysis, Environ Health Perspect, 128, 66001, https://doi.org/10.1289/EHP5312, 2020.
Hersbach, H., Bell, B., Berrisford, P., Hirahara, S., Horanyi, A., Muñoz-Sabater, J., Nicolas, J., Peubey, C., Radu, R., Schepers, D., Simmons, A., Soci, C., Abdalla, S., Abellan, X., Balsamo, G., Bechtold, P., Biavati, G., Bidlot, J., Bonavita, M., De Chiara, G., Dahlgren, P., Dee, D., Diamantakis, M., Dragani, R., Flemming, J., Forbes, R., Fuentes, M., Geer, A., Haimberger, L., Healy, S., Hogan, R. J., Hólm, E., Janisková, M., Keeley, S., Laloyaux, P., Lopez, P., Lupu, C., Radnoti, G., de Rosnay, P., Rozum, I., Vamborg, F., Villaume, S., and Thépaut, J. N.: The ERA5 global reanalysis, Quarterly Journal of the Royal Meteorological Society, 146, 1999-2049, https://doi.org/10.1002/qj.3803, 2020.
Huang, J., Wang, T., Wang, W., Li, Z., and Yan, H.: Climate effects of dust aerosols over East Asian arid and semiarid regions, Journal of Geophysical Research: Atmospheres, 119, 11398-11416, https://doi.org/10.1002/2014jd021796, 2014.
Jickells, T. and Moore, C. M.: The Importance of Atmospheric Deposition for Ocean Productivity, Annual Review of Ecology, Evolution, and Systematics, 46, 481-501, https://doi.org/10.1146/annurev-ecolsys-112414-054118, 2015.
Jickells, T. D., An, Z. S., Andersen, K. K., Baker, A. R., Bergametti, G., Brooks, N., Cao, J. J., Boyd, P. W., Duce, R. A., Hunter, K. A., Kawahata, H., Kubilay, N., laRoche, J., Liss, P. S., Mahowald, N., Prospero, J. M., Ridgwell, A. J., Tegen, I., and Torres, R.: Global iron connections between desert dust, ocean biogeochemistry, and climate, Science, 308, 67-71, https://doi.org/10.1126/science.1105959, 2005.
Kim, D., Chin, M., Cruz, C. A., Tong, D., and Yu, H.: Spring Dust in Western North America and Its Interannual Variability-Understanding the Role of Local and Transported Dust, Journal of Geophysical Research: Atmospheres, 126, e2021JD035383, https://doi.org/10.1029/2021jd035383, 2021.
Kim, D., Chin, M., Remer, L. A., Diehl, T., Bian, H., Yu, H., Brown, M. E., and Stockwell, W. R.: Role of surface wind and vegetation cover in multi-decadal variations of dust emission in the Sahara and Sahel, Atmospheric Environment, 148, 282-296, https://doi.org/10.1016/j.atmosenv.2016.10.051, 2017.
Kok, J. F., Ridley, D. A., Zhou, Q., Miller, R. L., Zhao, C., Heald, C. L., Ward, D. S., Albani, S., and Haustein, K.: Smaller desert dust cooling effect estimated from analysis of dust size and abundance, Nature Geoscience, 10, 274-278, https://doi.org/10.1038/ngeo2912, 2017.
Kong, S. S., Pani, S. K., Griffith, S. M., Ou-Yang, C. F., Babu, S. R., Chuang, M. T., Ooi, M. C. G., Huang, W. S., Sheu, G. R., and Lin, N. H.: Distinct transport mechanisms of East Asian

https://doi.org/10.5194/egusphere-2025-4589
Preprint. Discussion started: 5 October 2025

dust and the impact on downwind marine and atmospheric environments, Science of the Total Environment, 827, 154255, https://doi.org/10.1016/j.scitotenv.2022.154255, 2022.

Kurosaki, Y. and Mikami, M.: Threshold wind speed for dust emission in east Asia and its seasonal variations, Journal of Geophysical Research, 112, D17202, https://doi.org/10.1029/2006jd007988, 2007.

Li, Y., Mickley, L. J., and Kaplan, J. O.: Response of dust emissions in southwestern North America to 21st century trends in climate, CO2 fertilization, and land use: implications for air quality, Atmospheric Chemistry and Physics, 21, 57-68, https://doi.org/10.5194/acp-21-57-2021, 2021.

Liang, P., Chen, B., Yang, X., Liu, Q., Li, A., Mackenzie, L., and Zhang, D.: Revealing the dust transport processes of the 2021 mega dust storm event in northern China, Science Bulletin, 67, 21-24, https://doi.org/10.1016/j.scib.2021.08.014, 2022.

Molina, M. O., Gutiérrez, C., and Sánchez, E.: Comparison of ERA5 surface wind speed climatologies over Europe with observations from the HadISD dataset, International Journal of Climatology, 41, 4864-4878, https://doi.org/10.1002/joc.7103, 2021.

Mu, F. and Fiedler, S.: How much do atmospheric depressions and Mongolian cyclones contribute to spring dust activities in East Asia?, npj Climate and Atmospheric Science, 8, https://doi.org/10.1038/s41612-025-00929-w, 2025.

Pérez-Alarcón, A., Coll-Hidalgo, P., Trigo, R. M., Nieto, R., and Gimeno, L.: CyTRACK: An open-source and user-friendly python toolbox for detecting and tracking cyclones, Environmental Modelling & Software, 176, https://doi.org/10.1016/j.envsoft.2024.106027, 2024.

Pérez-Alarcón, A., Sorí, R., Fernández-Alvarez, J. C., Nieto, R., and Gimeno, L.: Comparative climatology of outer tropical cyclone size using radial wind profiles, Weather and Climate Extremes, 33, https://doi.org/10.1016/j.wace.2021.100366, 2021.

Piao, S., Wang, X., Park, T., Chen, C., Lian, X., He, Y., Bjerke, J. W., Chen, A., Ciais, P., Tømmervik, H., Nemani, R. R., and Myneni, R. B.: Characteristics, drivers and feedbacks of global greening, Nature Reviews Earth & Environment, 1, 14-27, https://doi.org/10.1038/s43017-019-0001-x, 2019.

Priestley, M. D. K., Ackerley, D., Catto, J. L., Hodges, K. I., McDonald, R. E., and Lee, R. W.: An Overview of the Extratropical Storm Tracks in CMIP6 Historical Simulations, Journal of Climate, 33, 6315-6343, https://doi.org/10.1175/jcli-d-19-0928.1, 2020.

Pu, B. and Ginoux, P.: Projection of American dustiness in the late 21(st) century due to climate change, Scientific Reports, 7, 5553-5563, https://doi.org/10.1038/s41598-017-05431-9, 2017.

Pu, B. and Ginoux, P.: Climatic factors contributing to long-term variations in surface fine dust concentration in the United States, Atmospheric Chemistry and Physics, 18, 4201-4215, https://doi.org/10.5194/acp-18-4201-2018, 2018.

Pu, B., Jin, Q., Ginoux, P., and Yu, Y.: Compound heat wave, drought, and dust events in California, Journal of Climate, 35, 1-42, https://doi.org/10.1175/jcli-d-21-0889.1, 2022.

Pu, B., Ginoux, P., Guo, H., Hsu, N. C., Kimball, J., Marticorena, B., Malyshev, S., Naik, V., O'Neill, N. T., Pérez García-Pando, C., Paireau, J., Prospero, J. M., Shevliakova, E., and Zhao, M.: Retrieving the global distribution of the threshold of wind erosion from satellite data and implementing it into the Geophysical Fluid Dynamics Laboratory land–atmosphere model (GFDL AM4.0/LM4.0), Atmospheric Chemistry and Physics, 20, 55-81, https://doi.org/10.5194/acp-20-55-2020, 2020.

https://doi.org/10.5194/egusphere-2025-4589
Preprint. Discussion started: 5 October 2025

Schenkel, B. A., Lin, N., Chavas, D., Oppenheimer, M., and Brammer, A.: Evaluating Outer Tropical Cyclone Size in Reanalysis Datasets Using QuikSCAT Data, Journal of Climate, 30, 8745-8762, https://doi.org/10.1175/jcli-d-17-0122.1, 2017.

Shaw, T. A., Baldwin, M., Barnes, E. A., Caballero, R., Garfinkel, C. I., Hwang, Y. T., Li, C., O'Gorman, P. A., Rivière, G., Simpson, I. R., and Voigt, A.: Storm track processes and the opposing influences of climate change, Nature Geoscience, 9, 656-664, https://doi.org/10.1038/ngeo2783, 2016.

Song, Q., Zhang, Z., Yu, H., Ginoux, P., and Shen, J.: Global dust optical depth climatology derived from CALIOP and MODIS aerosol retrievals on decadal timescales: regional and interannual variability, Atmospheric Chemistry and Physics, 21, 13369-13395, https://doi.org/10.5194/acp-21-13369-2021, 2021.

Tai, A. P. K., Ma, P. H. L., Chan, Y.-C., Chow, M.-K., Ridley, D. A., and Kok, J. F.: Impacts of climate and land cover variability and trends on springtime East Asian dust emission over 1982–2010: A modeling study, Atmospheric Environment, 254, 118348, https://doi.org/10.1016/j.atmosenv.2021.118348, 2021.

Tong, D. Q., Wang, J. X. L., Gill, T. E., Lei, H., and Wang, B.: Intensified dust storm activity and Valley fever infection in the southwestern United States, Geophys Res Lett, 44, 4304-4312, https://doi.org/10.1002/2017GL073524, 2017.

Wang, S., Yu, Y., Zhang, X.-X., Lu, H., Zhang, X.-Y., and Xu, Z.: Weakened dust activity over China and Mongolia from 2001 to 2020 associated with climate change and land-use management, Environmental Research Letters, 16, 124056, https://doi.org/10.1088/1748-9326/ac3b79, 2021.

Wohland, J., Folini, D., and Pickering, B.: Wind speed stilling and its recovery due to internal climate variability, Earth System Dynamics, 12, 1239-1251, https://doi.org/10.5194/esd-12-1239-2021, 2021.

Wu, C., Lin, Z., Shao, Y., Liu, X., and Li, Y.: Drivers of recent decline in dust activity over East Asia, Nature Communications, 13, 7105, https://doi.org/10.1038/s41467-022-34823-3, 2022.

Xi, X.: Revisiting the Recent Dust Trends and Climate Drivers Using Horizontal Visibility and Present Weather Observations, Journal of Geophysical Research: Atmospheres, 126, e2021JD034687, https://doi.org/10.1029/2021jd034687, 2021.

Xu, X., Levy, J. K., Zhaohui, L., and Hong, C.: An investigation of sand–dust storm events and land surface characteristics in China using NOAA NDVI data, Global and Planetary Change, 52, 182-196, https://doi.org/10.1016/j.gloplacha.2006.02.009, 2006.

Yang, H., Zhang, X., Zhao, F., Wang, J. a., Shi, P., and Liu, L.: Mapping Sand-dust Storm Risk of the World, in: World Atlas of Natural Disaster Risk, edited by: Shi, P., and Kasperson, R., Springer Berlin Heidelberg, Berlin, Heidelberg, 115-150, https://doi.org./10.1007/978-3-662-45430-5_7, 2015.

Yin, Z., Wan, Y., Zhang, Y., and Wang, H.: Why super sandstorm 2021 in North China?, National Science Review, 9, nwab16, https://doi.org/10.1093/nsr/nwab165, 2022.

Yu, H., Tan, Q., Chin, M., Remer, L. A., Kahn, R. A., Bian, H., Kim, D., Zhang, Z., Yuan, T., Omar, A. H., Winker, D. M., Levy, R., Kalashnikova, O., Crepeau, L., Capelle, V., and Chedin, A.: Estimates of African Dust Deposition Along the Trans-Atlantic Transit Using the Decade-long Record of Aerosol Measurements from CALIOP, MODIS, MISR, and IASI, Journal Of Geophysical Research-atmospheres, 124, 7975-7996, https://doi.org/10.1029/2019JD030574, 2019a.

https://doi.org/10.5194/egusphere-2025-4589
Preprint. Discussion started: 5 October 2025

Yu, Y. and Ginoux, P.: Assessing the contribution of the ENSO and MJO to Australian dust activity based on satellite- and ground-based observations, Atmospheric Chemistry and Physics, 21, 8511-8530, https://doi.org/10.5194/acp-21-8511-2021, 2021.

Yu, Y. and Ginoux, P.: Enhanced dust emission following large wildfires due to vegetation disturbance, Nature Geoscience, 15, 878-884, https://doi.org/10.1038/s41561-022-01046-6, 2022.

Yu, Y., Kalashnikova, O. V., Garay, M. J., and Notaro, M.: Climatology of Asian dust activation and transport potential based on MISR satellite observations and trajectory analysis, Atmospheric Chemistry and Physics, 19, 363-378, https://doi.org/10.5194/acp-19-363-2019, 2019b.

Zeng, Z., Ziegler, A. D., Searchinger, T., Yang, L., Chen, A., Ju, K., Piao, S., Li, L. Z. X., Ciais, P., Chen, D., Liu, J., Azorin-Molina, C., Chappell, A., Medvigy, D., and Wood, E. F.: A reversal in global terrestrial stilling and its implications for wind energy production, Nature Climate Change, 9, 979-985, https://doi.org/10.1038/s41558-019-0622-6, 2019.

Zong, Q., Mao, R., Gong, D.-Y., Wu, C., Pu, B., Feng, X., and Sun, Y.: Changes in Dust Activity in Spring over East Asia under a Global Warming Scenario, Asia-Pacific Journal of Atmospheric Sciences, 57, 839-850, https://doi.org/10.1007/s13143-021-00224-7, 2021.